Capacity and Energy Efficiency Trade-off in Multi-Packet Reception Wireless Systems

Ayman T. Abusabah [†‡] and Rodolfo Oliveira[†‡]
[†]Departamento de Engenharia Electrotécnica, Faculdade de Ciências e Tecnologia, FCT,
Universidade Nova de Lisboa, 2829-516 Caparica, Portugal
[‡]IT, Instituto de Telecomunicações, Portugal
emails: a.sabah@campus.fct.unl.pt, rado@fct.unl.pt

***Abstract*—The radio access in Internet-of-Things (IoT) networks requires minimizing the energy consumption while achieving the capacity requirements especially for high density deployment. The Multi-Packet Reception (MPR) systems can potentially increase the capacity of devices due to the capability of decoding multiple transmitted packets at the receiver. However, the aggregate interference in such scenarios can lead to unfair distribution of the resources and eventually waste of energy. Therefore, this work provides an analytical characterization of the trade-off between capacity and energy consumption while regulating the channel access of multiple transmitters to a single-MPR receiver. The theoretical modeling considers different densities of spatially distributed nodes and their channel propagation conditions, in addition to different capture sensitivity thresholds at the receiver. The model is validated through simulation and it is shown to be an effective tool to identify the optimal channel access probability that maximizes the capacity per energy consumption.**

***Keywords*—Internet-of-Thing (IoT), Multi-packet Reception (MPR), Energy Efficiency, Performance Analysis.**

I. Introduction

WITH the tremendous development of Internet-of-Things (IoT), tens of thousands of IoT devices are expected to access the network for data transmission. It is agreed that new specific radio access protocols are required to support the deployment of high-density IoT networks [1]. The radio access in IoT networks necessitates new features mainly minimizing the energy consumption while maintaining massive connectivity support of devices. In such scenarios, the devices, e.g., sensors, smart cities, etc, have very relaxed requirements on capacity and spend the vast majority of their lifetime in idle mode as most of the IoT applications only require the infrequent transmission of short packets.

This has motivated several research studies and standardization initiatives in supporting a massive number of radio-connected devices. Low-power wide-area network (LPWAN) is a wireless wide area network technology designed specifically for high-density devices with low-bandwidth and battery consumption limits to operate at low bit rates over long ranges. Traditional cellular network operators have offered commercial LPWAN technologies in licensed bands, e.g., LTE enhancements for machine-type communications (eMTC), extended coverage GSM (EC-GSM), and Narrowband IoT (NB-IoT) [2]. On the other hand, proprietary LPWAN technologies, e.g., Sigfox, LoRa, and Ingenu, have acquired interest due to the lower operational costs in nonlicensed bands and the deployment flexibility [3], [4].

In highly dense IoT networks, the adopted medium access control (MAC) techniques and connection management play a crucial role in optimizing the network parameters. The coordination is exacerbated in case of high dense scenarios where the ongoing transmission interferes with other transmissions, leading eventually to packet loss that could be handled by appropriate retransmission mechanisms at the expense of waste of resources and more power consumption [5]. Consequently, unconventional MAC solutions were adopted in the so-called IoT [6], where nodes can operate in energy-constrained scenarios, i.e., up to 10 years of battery life for around 50 000 nodes per square kilometer.

Recent progress on physical-layer (PHY) communication technologies allows unprecedented throughput gains through the simultaneous reception of multiple packets including multi-user multiple input multiple output (MU-MIMO) and technologies, such as LoRa, a.k.a. multi-packet reception (MPR) [7]. Usually, the MAC policies of MPR are designed based on the optimal number of transmitters that maximize the capacity of the PHY-layer without considering the energy consumption constraint. Therefore, this work provides analytical modeling of the trade-off between the capacity and energy consumption based on a distributed MAC scheme considering different access probabilities of multiple transmitters to a single-MPR receiver.

The energy consumption for energy-limited wireless sensors and ad hoc networks has been studied in [8]. The authors have defined the maximum total number of bits that the network can deliver per Joule of energy. The work in [9] has considered the capacity and energy efficiency of training-based communication assuming imperfect channel estimation due to randomness in channel conditions. The authors in [10] have developed a model capturing the effect of PHY layer parameters to analyze energy-efficient communications. In ultra-dense Networks (UDNs), there has also been a growing effort on optimizing the energy consumption [11]–[15]. The authors in [11] have discussed various approaches to handle energy efficiency problems in UDNs, ranging from deployment to optimization. In [12], the authors have derived the ergodic capacity of the uplink UDN. The analyses in [13], [14] have considered the coverage probability and throughput of downlink UDNs

under saturated traffic assumption. A novel cross-layer analytical model to capture the unsaturated traffic of UDN in the presence of quality of service (QoS) requirements has been proposed in [15].

For sake of providing a more realistic and representative practical network scenario, the proposed analysis of capacity and power consumption trade-off considers stochastic modeling for the spatial distribution of the communicating nodes besides the fading propagation channels. The proposed modeling is based on a distributed MAC scheme considering different access probabilities of multiple transmitters to a single-MPR receiver. The importance of this work comes from the capability of regulating the access of concurrent transmissions while trading-off capacity for energy efficiency based on the user requirements and network scenarios.

We use the following notations in the paper: $\mathbb{P}[X = x]$ is the probability of a random variable (RV) X. $f_X(.)$ and $F_X(.)$ represent the probability density function (PDF) and the cumulative density function (CDF), respectively. $\mathrm{E}[X]$ denote the expectation. The moment generating function (MGF) of the RV X is represented by Φ_X. Gamma(k, θ) is the Gama distribution where k and θ represent the shape and scale parameters, respectively. The Gamma function and the incomplete gamma function are given by $\Gamma(x)$ and $\Gamma(p, x)$, respectively. ${}_2\mathrm{F}_1(a, b; c; z)$ is the Gauss Hypergeometric function.

II. System Model and Assumptions

A. Network Model

The network scenario is shown in Fig. 1 where we model the locations of communicating nodes by independent homogeneous Poisson point processes (PPPs) in $\mathbb{R}^2$. The homogeneous PPP has shown high accuracy in modeling the position of the nodes in both static and mobile scenarios [16], [17]. Given that N is a RV representing the number of nodes located within an area $|A|$, the probability that $\mathbb{P}[N(|A|) = n]$ is given by

$$\mathbb{P}[N(|A|) = n] = \frac{(\lambda|A|\tau)^n}{n!} e^{-\lambda|A|\tau}, \tag{1}$$

where λ is a constant representing the density of the nodes per unit area (nodes/m^2) and τ represents the channel access probability depending on the adopted MAC protocol and/or policies. We condition on a reference receiving node, Rx_o, at the center of a Cartesian space being communicating with an i-th transmitting node Tx_i, which results in a homogeneous PPP with the corresponding density [18]. Therefore, the aggregate interference is attributed to the nodes bounded by the inner raduis $R_{\mathcal{I}}$ and the outer radius $R_{\mathcal{O}}$ in the area $A = \pi(R_{\mathcal{O}}^2 - R_{\mathcal{I}}^2)$.

B. Communication Model

We attribute the variations in the envelope of the received signal power to both large-scale fading and small-scale fading, given as follows

$$P_i^r = P_i^t h_i r_i^{-\alpha}, \tag{2}$$

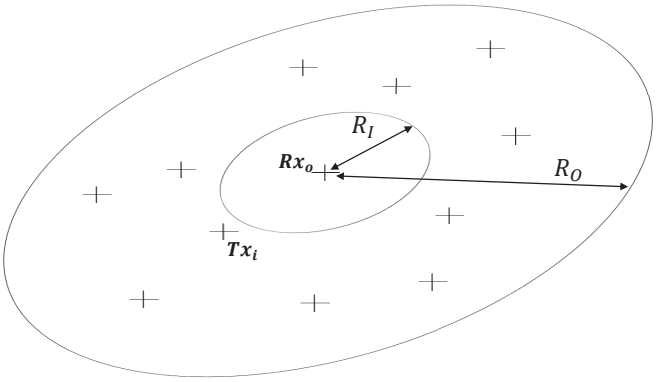

Fig. 1. Network model scenario.

where P_i^t represents the power of the transmitted signal by the i-th node, h_i denotes the fading channel gain between the i-th node and the reference receiver, $r_i > 1$ is the distance to Rx_o from the i-th node, and $\alpha > 2$ is the propagation loss coefficient. We highlight that h_i and r_i represent instant values of the RVs H_i and R_i, respectively.

C. Channel model

We adopt the Gamma distribution to approximate the power of the fading channel, i.e., $H_i \sim$ Gamma(k, θ). The Gamma distribution can effectively approximate the stochastic power fading when there is no line-of-sight (LoS) as in the Rayleigh fading channel or the LoS link as in the Rician fading channel [19]. Particularly, the fading power of a Rayleigh channel is drawn from the exponential distribution with mean $\frac{1}{\mu}$, which can be then represented by the Gamma distribution as follows

$$H_i^{Ray} \sim \text{Gamma}(k = 1, \theta = \frac{1}{\mu}). \tag{3}$$

Furthermore, the Rician fading channel can be described through the parameters K and Ω where K represents the ratio between the LoS power component and the non-LoS power components, and Ω denotes the total power from both components. Consequently, the received signal amplitude is described by the Rician distribution with parameters $\nu^2 = \frac{K\Omega}{1+K}$ and $\sigma^2 = \frac{\Omega}{2(1+K)}$. The value of K in decibels is $K_{dB} = 10\log_{10}(K)$. For $X \sim Rice(\nu, \sigma)$, then, $\left(\frac{X}{\sigma}\right)^2 \sim \chi^2\left(m = 2, \beta = \frac{\nu}{\sigma}\right)$ is a non-central Chi-squared distribution where m and β are the degrees of freedom and non-centrality parameter, respectively. Thereafter, moment matching is used to approximate H_i^{Rice} for a Gamma distribution as follows

$$H_i^{Rice} \sim \text{Gamma}\left(k = \frac{(\nu^2 + 2\sigma^2)^2}{4\sigma^2(\nu^2 + \sigma^2)}, \theta = \frac{4\sigma^2(\nu^2 + \sigma^2)}{(\nu^2 + 2\sigma^2)^2}\right), \tag{4}$$

The homogeneity of the nodes' distribution over $A = \pi(R_{\mathcal{O}}^2 - R_{\mathcal{I}}^2)$ leads to

$$f_{R_i}(r) = \frac{2r}{((R_{\mathcal{O}}^2 - R_{\mathcal{I}}^2))}, R_{\mathcal{I}} < r < R_{\mathcal{O}}. \tag{5}$$

Consequently, the PDF of $L_i = R_i^{-\alpha}$ is found as follows

$$f_{L_i}(l) = -\frac{2l^{\frac{-2}{\alpha}-1}}{\alpha(R_{\mathcal{O}}^2 - R_{\mathcal{I}}^2)}, R_{\mathcal{O}}^{-\alpha} < l < R_{\mathcal{I}}^{-\alpha}. \quad (6)$$

D. MPR Capture Condition

We denote the received SINR at node Rx_o by γ_i, given as follows

$$\gamma_i = \frac{P_{i,o}^r}{Y}, \quad (7)$$

where $P_{i,o}^r = P_i^t h_{i,o} r_{i,o}^{-\alpha}$ is the intended received power at the reference node due to the transmission of Tx_i node. $Y = I + \sigma_N^2$ where $I = \sum_{i=1, i\in\mathcal{I}}^{N} P_i^r$ represents the aggregate interference power generated by the other nodes when a signal is to be decoded from a corresponding transmitter given that P_i^r's are independent and identically distributed (i.i.d.) RVs. The noise power is defined as $\sigma_N^2(\text{dBm}) = -174 + 10\log_{10}(\text{BW}) + \mathcal{F}$, where $\sigma_N^2 = 10^{\sigma_N^2(\text{dBm})/10}$, $\mathcal{F}$ represents the noise figure, BW denotes the utilized bandwidth, and 174 dBm/Hz is the reference noise level at room temperature.

The performance of the MPR receiver is usually measured by the capture condition ($\gamma_i > b$) [20] where b is the capture threshold that specifies the receiver's sensitivity. The condition $b > 1$ represents Single-Packet Reception (SPR) receivers, while $b < 1$ represents MPR receivers adopting CDMA [21]. Consequently, the successfully MPR reception is conditioned on the SINR greater than the capture condition as follows

$$P_{Succ}(b) = \mathbb{P}[\gamma_i > b] = 1 - F_{\gamma_i}(b). \quad (8)$$

III. Computation on P_{Succ}

A. Characterization on $P_{i,o}^r$

The distribution of the RV $P_{i,o}^r$ is described by the scalar P_i^t and the RVs $H_{i,o}$ and $L_{i,o}$. Given that X follows a Gamma distribution, then, $cX \sim \text{Gamma}(k, c\theta)$, $c > 0$, yielding

$$f_{\mathcal{H}_i}(h) = \frac{h^{k-1}e^{-\frac{h}{\vartheta}}}{\vartheta^k \Gamma(k)}, \quad (9)$$

where $\mathcal{H}_i = P_i^t H_i$ and $\vartheta = P_i^t \theta$. Assuming that $\mathcal{H}_i$ and L_i are independent RVs, the product distribution can then be used to obtain the PDF of $P_{i,o}^r$ as follows

$$f_{P_{i,o}^r}(x) = \int_{-\infty}^{\infty} \frac{1}{|l|} f_{\mathcal{H}_i}(x/l) f_{L_i}(l) dl, \quad (10)$$

which can be solved by substituting $f_{\mathcal{H}_i}(x/l)$ by (9) and $f_{L_i}(l)$ by (6), yielding to

$$f_{P_{i,o}^r}(x) = \int_{R_{\mathcal{O}}^{-\alpha}}^{R_{\mathcal{I}}^{-\alpha}} -\frac{1}{|l|} \frac{(x/l)^{k-1} e^{\frac{-ls}{\vartheta}}}{\Gamma(k)\vartheta^k} \frac{2l^{\frac{-2}{\alpha}-1}}{\alpha(R_{\mathcal{O}}^2 - R_{\mathcal{I}}^2)} dl. \quad (11)$$

By solving the integral in (11) we obtain

$$f_{P_{i,o}^r}(x) = \left(\Gamma\left[k + \frac{2}{\alpha}, \frac{R_{\mathcal{I}}^{\alpha} x}{\vartheta}\right] - \Gamma\left[k + \frac{2}{\alpha}, \frac{R_{\mathcal{O}}^{\alpha} x}{\vartheta}\right]\right) \times \frac{2x^{-\frac{2+\alpha}{\alpha}} \vartheta^{\frac{2}{\alpha}}}{\alpha(R_{\mathcal{O}}^2 - R_{\mathcal{I}}^2)\Gamma(k)}. \quad (12)$$

Therefore, the moment generation function (MGF) of $P_{i,o}^r$, defined as $\Phi_{P_{i,o}^r}(s) = \text{E}[e^{sP_{i,o}^r}]$ is given by

$$\Phi_{P_{i,o}^r}(s) = \frac{R_{\mathcal{O}}^2 \varrho_1(R_{\mathcal{O}}^{-\alpha} s\vartheta) - R_{\mathcal{I}}^2 \varrho_1(R_{\mathcal{I}}^{-\alpha} s\vartheta)}{R_{\mathcal{O}}^2 - R_{\mathcal{I}}^2}, \quad (13)$$

where $\varrho_1(x) = {}_2\text{F}_1(k, \frac{-2}{\alpha}, \frac{-2+\alpha}{\alpha}, x)$.

B. Characterization of I

In this section, we characterize the aggregate interference I. The RV I is merely the summation of N independent RVs, i.e., ($I = P_1^r + P_2^r + ... + P_N^r$) where N has already defined in (1).

Since P_i^r's are assumed to be independent, then for n active interferers, we get

$$\Phi_{I|n}(s) = \left(\Phi_{P_i^r}(s)\right)^n. \quad (14)$$

The distribution of I can be then expressed as follows

$$f_I(j) = \sum_{n=0}^{\infty} f_I(j|N=n)\mathbb{P}[N=n]. \quad (15)$$

Departing from (14), the MFG of I, $\Phi_I(s)$, can be obtained as follows

$$\Phi_I(s) = \sum_{n=0}^{\infty} P[N=n]\Phi_{I|n}(s). \quad (16)$$

Using (1) and (14), the MGF of I is derived as follows

$$\Phi_I(s) = \sum_{n=0}^{\infty} \frac{\left(\lambda|A|\tau\Phi_{P_i^r}(s)\right)^n}{n!} e^{-\lambda|A|\tau} = e^{\lambda|A|\tau(\Phi_{P_i^r}(s)-1)}. \quad (17)$$

The MGF obtained in (17) can be used to find the x-th moment of I, i.e., $\text{E}[I^x] = \frac{d^x}{ds^x}\Phi_I(s)|_{s=0}$. For the approximation of Y, the simulated aggregate interference is compared with different known distributions to identify the best distribution that fits the sample data. The test results show that the Gamma distribution can effectively approximate the aggregate interference Y which is aligned with simulation results demonstrated in Section IV. Furthermore, the results in [22] emphasize this observation where the Gamma distribution shows high accuracy in approximating the aggregate interference in channel fading conditions.

Thus, we use the Gamma distribution for the approximation of the RV Y as follows

$$f_Y(y) = \frac{y^{k_{eq}-1} e^{\frac{-y}{\theta_{eq}}}}{\theta_{eq}^{k_{eq}} \Gamma(k_{eq})}, \quad \text{for } y > 0, \quad (18)$$

where

$$k_{eq} = \frac{\text{E}[Y]^2}{\text{E}[Y^2] - \text{E}[Y]^2}, \text{ and } \quad \theta_{eq} = \frac{\text{E}[Y^2] - \text{E}[Y]^2}{\text{E}[Y]}, \quad (19)$$

are shape and scale parameters, respectively, with $\text{E}[Y] = \text{E}[I] + \sigma_N^2$, $\text{E}[Y^2] = E[I^2] + 2\sigma_N^2\text{E}[I] + (\sigma_N^2)^2$, and $\text{E}[I]$ and $\text{E}[I^2]$ are given in (20a) and (20b), respectively.

$$\mathrm{E}[I] = \frac{2AkR_{\mathcal{I}}^{-\alpha}R_{\mathcal{O}}^{-\alpha}\left(R_{\mathcal{I}}^{\alpha}R_{\mathcal{O}}^{2} - R_{\mathcal{I}}^{2}R_{\mathcal{O}}^{\alpha}\right)\vartheta\lambda\tau}{\left(R_{\mathcal{I}}^{2} - R_{\mathcal{O}}^{2}\right)(-2+\alpha)} \tag{20a}$$

$$\mathrm{E}[I^2] = \frac{Ak\vartheta\lambda\tau}{\left(R_{\mathcal{I}}^{2} - R_{\mathcal{O}}^{2}\right)^2}\left(\frac{(1+k)(R_{\mathcal{I}}R_{\mathcal{O}})^{-2\alpha}\left(R_{\mathcal{I}}^{2} - R_{\mathcal{O}}^{2}\right)\left(R_{\mathcal{I}}^{2\alpha}R_{\mathcal{O}}^{2} - R_{\mathcal{I}}^{2}R_{\mathcal{O}}^{2\alpha}\right)}{-1+\alpha} + \frac{4Ak\left(R_{\mathcal{I}}^{2-\alpha} - R_{\mathcal{O}}^{2-\alpha}\right)^2\lambda\tau}{(-2+\alpha)^2}\right) \tag{20b}$$

C. Computation of P_{Succ}

Departing from (8) and given that $P_{i,o}^{r}$ and Y are independent RVs, P_{Succ} can be solved as follows

$$P_{Succ}(b) = 1 - \int_{0}^{b}\int_{0}^{\infty} y f_{P_{i,o}^{r}}(yz) f_{Y}(y) dy dz. \tag{21}$$

Substituting $P_{i,o}^{r}$ and Y by (12) and (18), respectively, yields to a closed-form expression given by (22), where $\varrho_2(x) = {}_2\mathrm{F}_1(k_{eq}, k+k_{eq}, 1+k_{eq}, x)$, and $\varrho_3(x) = {}_2\mathrm{F}_1(k+k_{eq}, k_{eq}-\frac{2}{\alpha}, 1+k_{eq}-\frac{2}{\alpha}, x)$.

D. Average Number of Success transmissions

Given that the N nodes are spatially i.i.d., then, the expected number of successfully captured packets at node Rx_o can be approximated as follows

$$E_{RX}(b) \simeq \mathrm{E}[N]P_{Succ}(b) = \lambda A\tau P_{Succ}(b). \tag{23}$$

E. Capacity and Energy Consumption

We define energy consumption as the amount of successfully transmitted power in a unit of time, given as follows

$$E_{Con} = \mathrm{E}[N]P_{i}^{t}t = \lambda A\tau P_{i}^{t}t. \tag{24}$$

The network capacity is defined in terms of E_{RX}, which represents the average rate successfully received for a specific capture condition, b, i.e., $C = E_{RX}\mathrm{BW}\log_2(1+b)$. Therefore, the capacity per energy consumption can be formulated as follows

$$C_{Con} = \frac{C}{E_{Con}\mathrm{BW}} \simeq \frac{P_{Succ}(b)\log_2(1+b)}{P_{i}^{t}t}. \tag{25}$$

IV. Performance Analysis

The simulation is based on the comparison between the theoretical derivations and the Monte Carlo simulations. The theoretical results were generated using the expressions derived in III-D and III-E. The simulation results were obtained by averaging 10^6 realizations of the stochastic process generated in *MATLAB* according to the parameters listed in Table I and Table II.

TABLE I
NETWORK PARAMETERS.

Symbol	Value	Symbol	Value
$R_{\mathcal{I}}$	1 m	$R_{\mathcal{O}}$	5 m
λ	$\{3, 5, 15\}$ nodes/m^2	b	{0.3, 0.4, 0.5}

TABLE II
CHANNEL PARAMETERS.

Symbol	Value	Symbol	Value
μ	1	α	4
P_i^t	1 Watt	BW	1 Hz
σ_N^2	0	t	1 s

The theoretical and simulated results for the number of successfully received transmissions, E_{RX}, versus the receiver capture threshold, b, are depicted in Fig. 2 considering different access probabilities $\tau = \{0.8, 0.9, 1.0\}$. A comparison between the simulated data and the theoretical derivations indicates the high accuracy of the proposed approximation. The parameter b determines the receiver's capability on sensing the ongoing transmissions. Therefore, the results clearly show that E_{RX} is decreased by increasing the capture condition b. Moreover, the results indicate an increase in E_{RX} when adopting higher τ values which can be attributed due to the higher number of granted nodes to access the channel.

Fig. 3 plots the capacity per energy consumption C_{Con} versus the access probability τ for different capture conditions, b, and network densities, λ. As can be seen, for each scenario there is an optimal number of simultaneous transmissions determined by a specific τ value that maximizes the capacity per energy consumption. The results indicate that the increase in τ is beneficial up to an optimal value. After that, the performance degrades with the increase of τ, which can be justified due to the increase in the interference when considering more concurrent transmissions and due to the increase in energy consumption. This also highlights the importance of the channel access mechanism in optimizing the network performance by deciding on the

$$\begin{aligned} P_{Succ}(b) = & 1 - \frac{(R_{\mathcal{I}}R_{\mathcal{O}})^{-k_{eq}\alpha}(b\theta_{eq})^{-k_{eq}}\vartheta^{k_{eq}}}{\left(R_{\mathcal{I}}^{2} - R_{\mathcal{O}}^{2}\right)}\left(R_{\mathcal{I}}^{2}R_{\mathcal{O}}^{k_{eq}\alpha}\left(\frac{bR_{\mathcal{I}}^{\alpha}\theta_{eq}}{\vartheta}\right)^{k_{eq}} - R_{\mathcal{I}}^{k_{eq}\alpha}R_{\mathcal{O}}^{2}\left(\frac{bR_{\mathcal{O}}^{\alpha}\theta_{eq}}{\vartheta}\right)^{k_{eq}} + \frac{1}{(-2+k_{eq}\alpha)}\right. \\ & \left.\frac{1}{\Gamma[k]\Gamma[1+k_{eq}]}\Gamma[k+k_{eq}]\left(-R_{\mathcal{I}}^{2}R_{\mathcal{O}}^{k_{eq}\alpha}(-2+k_{eq}\alpha)\varrho_2\left(-\frac{R_{\mathcal{I}}^{-\alpha}\vartheta}{b\theta_{eq}}\right) + k_{eq}R_{\mathcal{I}}^{2}R_{\mathcal{O}}^{k_{eq}\alpha}\alpha\varrho_3\left(-\frac{R_{\mathcal{I}}^{-\alpha}\vartheta}{b\theta_{eq}}\right) + \right.\right. \\ & \left.\left. R_{\mathcal{I}}^{k_{eq}\alpha}R_{\mathcal{O}}^{2}\left((-2+k_{eq}\alpha)\varrho_2\left(-\frac{R_{\mathcal{O}}^{-\alpha}\vartheta}{b\theta_{eq}}\right) - k_{eq}\alpha\varrho_2\left(-\frac{R_{\mathcal{O}}^{-\alpha}\vartheta}{b\theta_{eq}}\right)\right)\right)\right) \end{aligned} \tag{22}$$

optimal number of concurrent transmissions that an MPR receiver can handle depending on its capture threshold value. Moreover, the results indicate that the optimal τ needed to maximize the performance is decreased when adopting a higher network density scenario, i.e., $\tau \simeq 0.05$ for $\lambda = 15$ and $\tau \simeq 0.25$ for $\lambda = 3$. The results highlight that the optimal access probability is determined by the imposed interference that is a function of the node's density and the receiver capture probability.

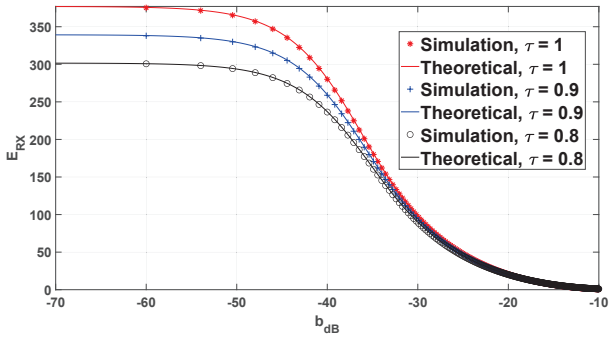

Fig. 2. Number of successfully received transmissions versus capture threshold considering different access probabilities for $\lambda = 5$.

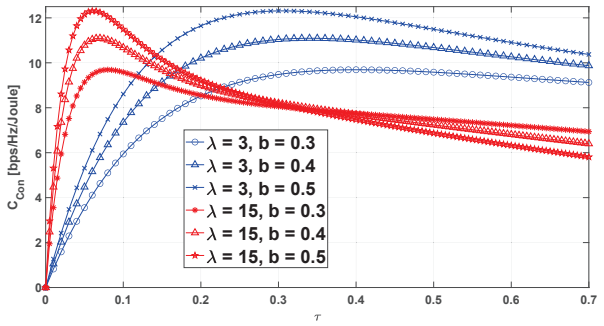

Fig. 3. Capacity per energy consumption versus access probability considering different capture thresholds and transmitter densities.

V. Conclusions

In this paper, we have characterized the energy efficiency and capacity trade-off considering different access probabilities of distributed transmitters to a single-MPR receiver. The simulated results validate the analytical derivations and highlight the importance of channel access in optimizing the capacity per energy consumption depending on the network density and the receiver capture condition.

The analysis of the trade-off between the capacity and energy efficiency indicates that there is always an optimal point of operation in terms of the achieved capacity-energy efficiency pair. This indicates that future radio networks and techniques should be designed very carefully to consider more efficient solutions from the energy point of view not only due to societal reasons but also due to the increased operational costs to the network operators.

Acknowledgements

This work has received funding from the European Union's Horizon 2020 research and innovation programme under the Marie Skłodowska-Curie ETN TeamUp5G, grant agreement No. 813391, and partially funded by *Fundação para a Ciência e Tecnologia* under the project UIDB/50008/2020.

References

[1] Lalit Chettri and Rabindranath Bera. A Comprehensive Survey on Internet of Things (IoT) Toward 5G Wireless Systems. *IEEE Internet Things J.*, 7(1):16–32, 2020.

[2] Olof Liberg, Marten Sundberg, Y.-P. Eric Wang, Johan Bergman, and Joachim Sachs. Chapter 7 - NB-IoT. In *Cellular Internet of Things*, pages 217–296. Academic Press, 2018.

[3] A Survey on LPWA Technology: LoRa and NB-IoT. *ICT Express*, 3(1):14–21, 2017.

[4] Daniele Croce, Michele Gucciardo, Stefano Mangione, Giuseppe Santaromita, and Ilenia Tinnirello. LoRa Technology Demystified: From Link Behavior to Cell-Level Performance. *IEEE Trans. Wireless Commun.*, 19(2):822–834, 2020.

[5] I. Demirkol, C. Ersoy, and F. Alagoz. MAC Protocols for Wireless Sensor Networks: A Survey. *IEEE Commun. Mag.*, 44(4):115–121, 2006.

[6] Abdelmalik Bachir, Mischa Dohler, Thomas Watteyne, and Kin K. Leung. MAC Essentials for Wireless Sensor Networks. *Commun. Surveys Tuts.*, 12(2):222–248, 2010.

[7] Lang Tong, Qing Zhao, and G. Mergen. Multipacket Reception in Random Access Wireless Networks: From Signal Processing to Optimal Medium Access Control. *IEEE Commun. Mag.*, 39(11):108–112, 2001.

[8] Volkan Rodoplu and Teresa H. Meng. Bits-per-Joule Capacity of Energy-Limited Wireless Networks. *IEEE Trans. Wireless Commun.*, 6(3):857–865, 2007.

[9] Mustafa Cenk Gursoy. On the Capacity and Energy Efficiency of Training-Based Transmissions Over Fading Channels. *IEEE Trans. Inf. Theory*, 55(10):4543–4567, 2009.

[10] Farhad Mahmood, Erik Perrins, and Lingjia Liu. Energy-Efficient Wireless Communications: From Energy Modeling to Performance Evaluation. *IEEE Trans. Veh. Technol.*, 68(8):7643–7654, 2019.

[11] Amna Mughees, Mohammad Tahir, Muhammad Aman Sheikh, and Abdul Ahad. Energy-Efficient Ultra-Dense 5G Networks: Recent Advances, Taxonomy and Future Research Directions. *IEEE Access*, 9:147692–147716, 2021.

[12] Mahmoud Kamel, Walaa Hamouda, and Amr Youssef. Uplink Coverage and Capacity Analysis of mMTC in Ultra-Dense Networks. *IEEE Trans. Veh. Technol.*, 69(1):746–759, 2020.

[13] Abhishek K. Gupta, Xinchen Zhang, and Jeffrey G. Andrews. SINR and Throughput Scaling in Ultradense Urban Cellular Networks. *IEEE Wireless Commun. Lett.*, 4(6):605–608, 2015.

[14] Chang Li, Jun Zhang, and Khaled B. Letaief. Throughput and Energy Efficiency Analysis of Small Cell Networks with Multi-Antenna Base Stations. *IEEE Trans. Wireless Commun.*, 13(5):2505–2517, 2014.

[15] Yu Gu, Qimei Cui, Yu Chen, Wei Ni, Xiaofeng Tao, and Ping Zhang. Effective Capacity Analysis in Ultra-Dense Wireless Networks With Random Interference. *IEEE Access*, 6:19499–19508, 2018.

[16] Luis Irio, Antonio Furtado, Rodolfo Oliveira, Luis Bernardo, and Rui Dinis. Interference Characterization in Random Waypoint Mobile Networks. *IEEE Trans. Wireless Commun.*, 17(11):7340–7351, 2018.

[17] Ayman T. Abusabah, Md Arifur Rahman, Rodolfo Oliveira, and Adam Flizikowski. The Importance of Repetitions in Ultra-Dense NB-IoT Networks. *IEEE Commun. Lett.*, pages 1–1, 2022.

[18] F. Baccelli and B. Blaszczyszyn. *Stochastic Geometry and Wireless Networks*. Delft, The Netherlands: Now Publishers, Sep.2009.

[19] Ayman T. Abusabah, Luis Irio, Rodolfo Oliveira, and Daniel B. da Costa. Approximate Distributions of the Residual Self-Interference Power in Multi-Tap Full-Duplex Systems. *IEEE Wireless Commun. Lett.*, 10(4):755–759, 2021.

[20] Gam D. Nguyen, Anthony Ephremides, and Jeffrey E. Wieselthier. On Capture in Random-Access Systems. In *2006 IEEE International Symposium on Information Theory*, pages 2072–2076, 2006.

[21] B. Hajek, A. Krishna, and R.O. LaMaire. On The Capture Probability for A Large Number of Stations. *IEEE Trans. Commun.*, 45(2):254–260, 1997.

[22] Martin Haenggi and Radha Ganti. Interference in Large Wireless Networks. *Foundations and Trends in Networking*, 3:127–248, 01 2009.